Supplementary Material
Interaction between pentacene molecules and monolayer transition metal dichalcogenides

E. Black[1], P. Kratzer[2], and J. M. Morbec[1,*]

[1]School of Chemical and Physical Sciences, Keele University, Keele ST5 5BG, UK
[2]Fakultät für Physik, Universität Duisburg-Essen, Campus Duisburg, Lotharstr. 1, 47057 Duisburg, Germany
[*]Corresponding author: j.morbec@keele.ac.uk

1 Computational details

Table S1 summarises the computational details of the density-functional-theory calculations performed in this work.

Table S1: Computational details of the calculations performed in this work.

code	Quantum ESPRESSO[1,2]
theory	DFT[3]
exchange-correlation functional	GGA-PBE[4]
van der Waals method	Grimme's DFT-D3[5]
pseudopotentials	PAW[6,7]
	Mo.pbe-spn-kjpaw_psl.1.0.0.UPF,
	W.pbe-spn-kjpaw_psl.1.0.0.UPF,
	S.pbe-n-kjpaw_psl.1.0.0.UPF,
	Se.pbe-dn-kjpaw_psl.1.0.0.UPF,
	C.pbe-n-kjpaw_psl.1.0.0.UPF,
	H.pbe-kjpaw_psl.1.0.0.UPF
wavefunction energy cutoff	MoS_2: 80 Ry, $MoSe_2$: 100 Ry, WS_2: 80 Ry, WSe_2: 120 Ry
supercell	7×4, vacuum region: 40 Å
lattice parameters	MoS_2: 3.17 Å, $MoSe_2$: 3.30 Å, WS_2: 3.17 Å, WSe_2: 3.29 Å
k-point grid	$3 \times 6 \times 1$ Monkhorst–Pack grid[8]

2 Adsorption energies

Table S2 lists the difference in total energy between different adsorption sites and the most favorable site (top-Ch). Bridge sites: the central ring of pentacene lies over a bond between the transition metal (Mo or W) and the chalcogen atoms (S or Se); two different bridge configurations were investigated here: bridge A and bridge B, as they result in the atoms of the molecule being located in different sites on the TMD. Hollow site: the central ring of pentacene is on top of a hexagon in the TMD cell. Top-TM: the central ring of pentacene is on top of a transition metal (Mo or W) atom. Top-Ch: the central ring of pentacene is on top of chalcogen (S or Se) atom.

Table S2: Difference in total energy (in eV) between the different adsorption sites considered in this work and the most favorable one (top-Ch).

	Bridge-A	Bridge-B	Hollow	Top-TM	Top-Ch
MoS_2	0.079	0.003	0.049	0.046	0.000
$MoSe_2$	0.072	0.002	0.038	0.035	0.000
WSe_2	0.083	0.002	0.053	0.055	0.000
WSe_2	0.075	0.006	0.024	0.056	0.000

Table S3 lists the adsorption distances of pentacene/TMD heterostructures for different adsorption sites.

Table S3: Adsorption distances d (in Å) of pentacene/TMD heterostructures for different adsorption sites, calculated as the distance between the center of mass of the pentacene molecule and the center of mass of the top-chalcogen layer.

	Bridge-A	Bridge-B	Hollow	Top-TM
MoS_2	3.397	3.334	3.395	3.392
$MoSe_2$	3.475	3.415	3.463	3.459
WS_2	3.389	3.328	3.374	3.375
WSe_2	3.468	3.410	3.447	3.480

Contributions to the adsorption energy (E_{ads}):

$$E_{\text{ads}} = E_{\text{PEN/TMD}} - E_{\text{TMD}}^{\text{relax}} - E_{\text{PEN}}^{\text{iso-relax}} \tag{1}$$

due to the deformation of the molecule ($E_{\text{PEN}}^{\text{def}}$), deformation of the substrate ($E_{\text{TMD}}^{\text{def}}$), molecule-

molecule interaction ($E^{\mathrm{int}}_{\mathrm{PEN}}$) and molecule-substrate interaction ($E^{\mathrm{PEN}}_{\mathrm{TMD}}$) were calculated using[9]

$$E^{\mathrm{def}}_{\mathrm{PEN}} = E^{\mathrm{iso-adsgeom}}_{\mathrm{PEN}} - E^{\mathrm{iso-relax}}_{\mathrm{PEN}} \quad (2)$$

$$E^{\mathrm{def}}_{\mathrm{TMD}} = E^{\mathrm{adsgeom}}_{\mathrm{TMD}} - E^{\mathrm{relax}}_{\mathrm{TMD}} \quad (3)$$

$$E^{\mathrm{int}}_{\mathrm{PEN}} = E^{\mathrm{scell-adsgeom}}_{\mathrm{PEN}} - E^{\mathrm{iso-adsgeom}}_{\mathrm{PEN}} \quad (4)$$

$$E^{\mathrm{PEN}}_{\mathrm{TMD}} = E_{\mathrm{PEN/TMD}} - E^{\mathrm{adsgeom}}_{\mathrm{TMD}} - E^{\mathrm{scell-adsgeom}}_{\mathrm{PEN}} \quad (5)$$

where $E^{\mathrm{iso-relax}}_{\mathrm{PEN}}$ and $E^{\mathrm{iso-adsgeom}}_{\mathrm{PEN}}$ are the total energies of the isolated pentacene molecule (in a cubic supercell with lateral dimension of 48 Å) with relaxed and adsorbed geometries, respectively, while $E^{\mathrm{scell-adsgeom}}_{\mathrm{PEN}}$ is the total energy of the pentacene molecule in a 7×4 supercell with adsorbed geometry. Relaxed geometry means that all atoms were allowed to relax without the presence of the other component of the heterostructure; adsorbed geometry means that the geometry of the component was kept as it was obtained in the optimization of the geometry of the heterostructure. $E^{\mathrm{adsgeom}}_{\mathrm{TMD}}$ and $E^{\mathrm{relax}}_{\mathrm{TMD}}$ are the total energies of the monolayer TMD with adsorbed and relaxed geometry, respectively.

3 Electronic properties

Figure S1 displays the total density of states of isolated pentacene (pentacene molecule in a cubic supercell with lateral dimension of 48 Å) and isolated WSe_2, showing that the isolated systems have a type-II band alignment.

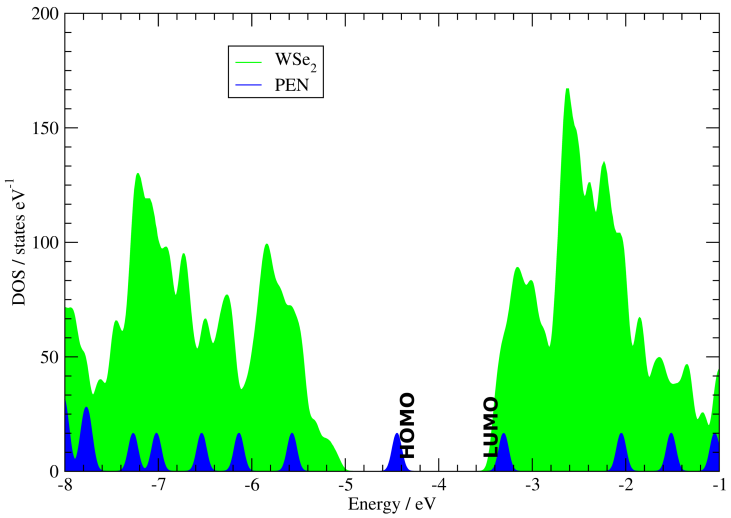

Figure S1: Total density of states (DOS) of isolated pentacene (in blue) and isolated monolayer WSe_2 (in green).

Figure S2 displays the total density of states of pentacene in three different states: isolated (molecule-molecule interaction is absent), in a 7×4 supercell without substrate (molecule-molecule interaction is present but molecule-substrate interaction is absent) and in the PEN/WSe_2 heterostructure (both molecule-molecule and molecule-substrate interactions are present). This

figure reveals the shift of pentacene HOMO and LUMO due to molecule-molecule and molecule-substrate interactions.

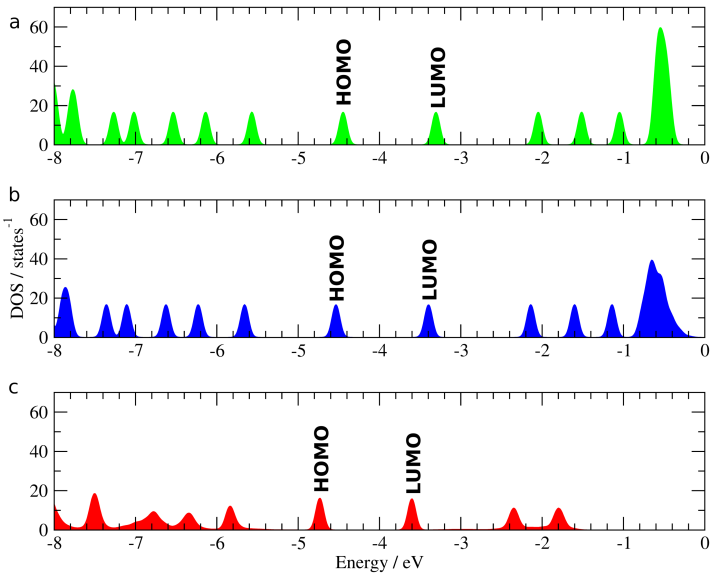

Figure S2: Total density of states (DOS) of pentacene in three different states: isolated (top panel, green), in a 7×4 supercell without substrate (middle panel, green) and in the PEN/WSe_2 heterostructure (bottom panel, red).

Table S4 lists the shifts of the HOMO and LUMO of single layer pentacene molecules when adsorbed on the TMDs, in comparison with the gas-phase state.

Table S4: Shifts (in meV) of the HOMO and LUMO positions of single layer pentacene molecules when adsorbed on the TMDs, in comparison with the gas-phase state. Negative values correspond to shifts to lower energies.

	PEN/MoS_2	PEN/$MoSe_2$	PEN/WS_2	PEN/WSe_2
HOMO (meV)	-321	-297	-300	-322
LUMO (meV)	-326	-322	-325	-292

Figure S3 displays the band structures of the heterostructures and the monolayer TMDs aligned with respect to the vacuum level.

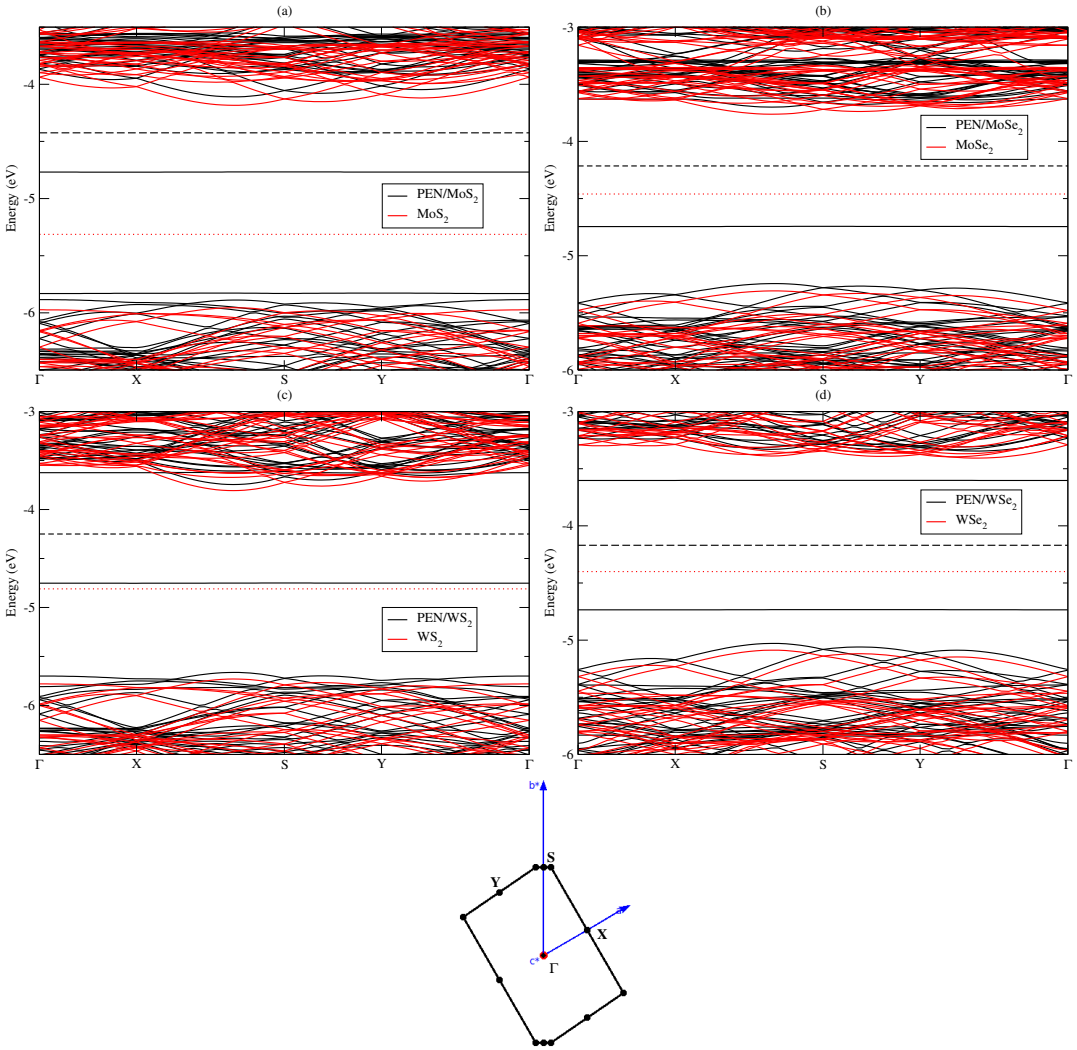

Figure S3: Band structures of the heterostructures (black curves) and the monolayer TMDs (red curves) aligned with respect to the vacuum level. (a) PEN/MoS_2, (b) PEN/$MoSe_2$, (c) PEN/WS_2, and (d) PEN/WSe_2. Black dashed and red dotted lines indicate the position of the Fermi level of the heterostrustures and the TMDs, respectively. The Brillouin zone of the supercell showing the symmetry points is displayed in the bottom panel.

Table S5 lists the position of the VBM and CBM of the TMDs (obtained using a 1×1 supercell) with and without SOC and the shifts caused by SOC.

Table S5: Positions of the VBM and CBM (in eV) of the TMDs, with respect to the vacuum level, obtained with (w/) and without (w/o) SOC. Shifts (Δ) listed here are the differences between the values with SOC and without SOC.

		w/o SOC	w/ SOC	Δ=(w/ SOC)−(w/o SOC)
MoS_2	VBM (eV)	-5.95	-5.88	+0.07
	CBM (eV)	-4.19	-4.28	-0.09
$MoSe_2$	VBM (eV)	-5.29	-5.06	+0.23
	CBM (eV)	-3.78	-3.75	+0.03
WS_2	VBM (eV)	-5.70	-5.53	+0.17
	CBM (eV)	-3.84	-4.01	-0.17
WSe_2	VBM (eV)	-5.07	-4.74	+0.33
	CBM (eV)	-3.41	-3.56	-0.15

4 Charge density

Fig. S4 shows the charge density difference between the heterostructure and isolated systems (Fig. S4), plotted on a plane cutting the long axis of the pentacene molecule and perpendicular to both molecule and TMD monolayer.

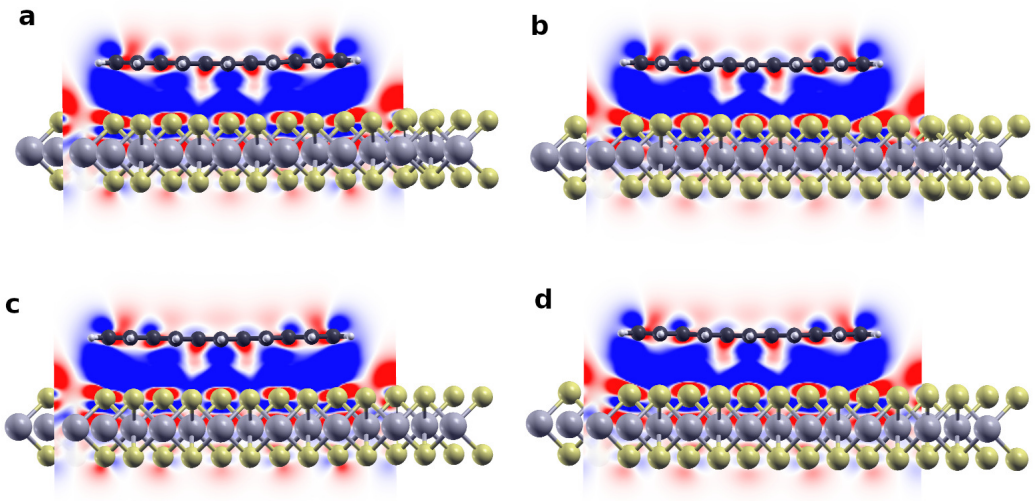

Figure S4: Charge density difference between the heterostructures ((a) PEN/MoS_2, (b) PEN/$MoSe_2$, (c) PEN/WS_2 and (d) PEN/WSe_2) and the isolated systems plotted on a plane perpendicular to both the pentacene molecule and the 2D TMD monolayer, cutting through the long axis of the molecule. Regions in blue and red represent depletion and accumulation of charge, respectively. Figure prepared using the XCrySDen software[10], with isovalues in the range of -0.00008 (blue) and +0.00008 (red) e/bohr^3.

References

[1] P. Giannozzi, S. Baroni, N. Bonini, M. Calandra, R. Car, C. Cavazzoni, D. Ceresoli, G. L. Chiarotti, M. Cococcioni, I. Dabo *et al.*, *Journal of physics: Condensed matter*, 2009, **21**, 395502.

[2] P. Giannozzi, O. Andreussi, T. Brumme, O. Bunau, M. B. Nardelli, M. Calandra, R. Car, C. Cavazzoni, D. Ceresoli, M. Cococcioni *et al.*, *Journal of physics: Condensed matter*, 2017, **29**, 465901.

[3] W. Kohn and L. J. Sham, *Phys. Rev.*, 1965, **140**, A1133–A1138.

[4] J. P. Perdew, K. Burke and M. Ernzerhof, *Physical review letters*, 1996, **77**, 3865.

[5] S. Grimme, J. Antony, S. Ehrlich and H. Krieg, *The Journal of chemical physics*, 2010, **132**, 154104.

[6] P. E. Blöchl, *Phys. Rev. B*, 1994, **50**, 17953–17979.

[7] *Quantum ESPRESSO pslibrary*, `http://pseudopotentials.quantum-espresso.org/legacy_tables/ps-library`.

[8] H. J. Monkhorst and J. D. Pack, *Phys. Rev. B*, 1976, **13**, 5188–5192.

[9] M. Müller, K. Diller, R. J. Maurer and K. Reuter, *The Journal of Chemical Physics*, 2016, **144**, 024701.

[10] A. Kokalj, *Journal of Molecular Graphics and Modelling*, 1999, **17**, 176–179.